IL NUOVO CIMENTO Vol. 31 C, N. 1 Gennaio-Febbraio 2008
DOI 10.1393/ncc/i2008-10281-9

The FLUKA code and its use in hadron therapy

G. Battistoni[1], F. Broggi[1], M. Brugger[2], M. Campanella[1][3], M. Carboni[4][3], F. Cerutti[2], P. Colleoni[5], C. D'Ambrosio[6][4], A. Empl[7], A. Fassò[8], Al. Ferrari[2], An. Ferrari[9], E. Gadioli[5], M. Lantz[10], K. Lee[11], G. Lukasik[2], A. Mairani[12][13], A. Margiotta[14], M. Mauri[2], M. C. Morone[15], A. Mostacci[16][4], S. Muraro[1], K. Parodi[13], V. Patera[16][4], M. Pelliccioni[4], L. Pinsky[7], J. Ranft[17], S. Roesler[2], S. Rollet[18], P. R. Sala[1], L. Sarchiapone[2], M. Sioli[14], G. Smirnov[2], F. Sommerer[2], C. Theis[2], S. Trovati[2], R. Villari[19][4], H. Vinke[2], V. Vlachoudis[2], T. Wilson[11] and N. Zapp[11]

([1]) *INFN, Sezione di Milano - Milano, Italy*
([2]) *CERN - Geneva, Switzerland*
([3]) *GARR Consortium - Rome, Italy*
([4]) *INFN, Laboratori Nazionali di Frascati - Frascati (RM), Italy*
([5]) *Università di Milano and INFN, Sezione di Milano - Milano, Italy*
([6]) *Università di Roma I - Rome, Italy*
([7]) *University of Houston - Houston, USA*
([8]) *SLAC - Standford, USA*
([9]) *CNAO - Pavia, Italy*
([10]) *Chalmers University of Technology - Göteborg, Sweden*
([11]) *NASA - Houston, USA*
([12]) *DKFZ - Heidelberg, Germany*
([13]) *HIT - Heidelberg, Germany*
([14]) *Università di Bologna and INFN, Sezione di Bologna - Bologna, Italy*
([15]) *Università di Roma II and INFN, Sezione di Roma II - Rome, Italy*
([16]) *Università "La Sapienza" - Rome, Italy*
([17]) *Siegen University - Siegen, Germany*
([18]) *ARC Seibersdorf Research, Austria*
([19]) *ENEA - Frascati (RM), Italy*

(ricevuto l' 11 Giugno 2008; pubblicato online il 17 Settembre 2008)

Summary. — FLUKA is a multipurpose Monte Carlo code describing transport and interaction with matter of a large variety of particles over a wide energy range in complex geometries. FLUKA is successfully applied in several fields, including, but not only, particle physics, cosmic-ray physics, dosimetry, radioprotection, hadron therapy, space radiation, accelerator design and neutronics. Here we briefly review recent model developments and provide examples of applications to hadron therapy, including calculation of physical and biological dose for comparison with analytical

treatment planning engines as well as β^+-activation for therapy monitoring by means of positron emission tomography.

PACS 25.70.Mn – Projectile and target fragmentation.
PACS 87.53.-j – Effects of ionizing radiation on biological systems.
PACS 87.55.K- – Monte Carlo methods.
PACS 87.57.uk – Positron emission tomography (PET).

1. – Introduction

The use of ion beams in external radiotherapy requires very accurate understanding of the complex processes of the ion interaction with matter, especially regarding the production of secondary particles and fragments. In fact, during irradiation, secondary neutrons, protons and heavier ions are produced and degrade the conformation of the dose delivered to the tumor by the primary beam while increasing the undesired burden to the healthy tissues outside the treated volume. In addition, some of the produced residues are β^+-active and can be detected by means of positron emission tomography (PET) to monitor the delivered treatment.

Hence, reliable nuclear models are an essential tool to achieve trustworthy dose and activity calculations in hadron therapy. In FLUKA [1, 2] nucleus-nucleus interactions at therapeutic energies are treated by an interface to a Relativistic Quantum Molecular Dynamics code (RQMD) [3] which can handle interactions down to about 100 MeV/n. The implementation of the Boltzmann Master Equation (BME) theory [4] for nucleus-nucleus interactions at lower energy is ongoing. For very light ions, namely from deuterons to alpha-particles, we are instead implementing an approach based on the already existing hadronic interaction model. This model, called PEANUT [5, 6], includes a detailed intranuclear cascade stage, coupled to pre-equilibrium and equilibrium particle emission. In this work, we briefly describe some important aspects related to the use of FLUKA in hadron therapy both with proton and carbon ions. A description of other FLUKA models and reports on extensive benchmarking can be found in [7] and citations therein as well as on the FLUKA website (`http://www.fluka.org`).

2. – Mixed radiation fields

In ion therapy nuclear reactions cause a significant alteration of the radiation field depending on the primary beam ion type and beam energy. For ions heavier than protons, this is shown mainly through a loss of primary beam particles (cf. fig. 1) and a build-up of secondary lower-charge fragments. Consequently, the dose distribution along the beam path is different compared to the dose profile resulting from the passage of primary ions in absence of nuclear interactions. In particular, the secondary lower-charge fragments, which have longer ranges than the primary beam, give rise to the characteristic dose tail beyond the Bragg peak (BP). FLUKA is being heavily benchmarked against models and experimental data concerning ion beams of interest for hadron therapy [10]. Figures 1 and 2 represent such a validation for a 400 MeV/n carbon beam on a water phantom [8, 9]. The depth dose profile calculated by FLUKA reproduces very well the experimental values in the entrance region and in the position of the BP (fig. 2) [9]. Both

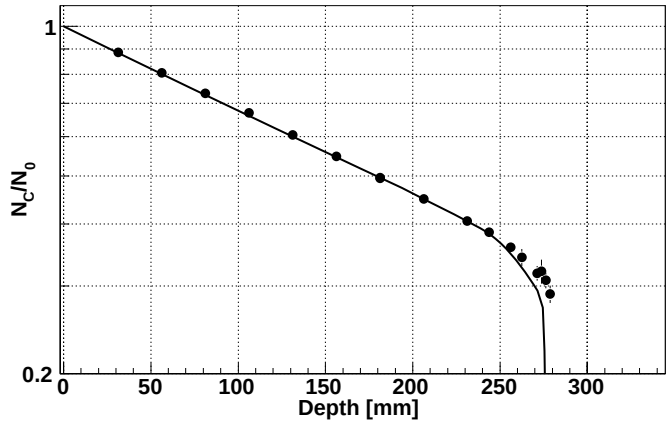

Fig. 1. – Beam attenutation profile (number of carbon ions N_C normalized to the primary beam ions N_0) as a function of depth in water for a 400 MeV/n carbon beam. The points [8] and the solid line [9] represent the experimental data and the FLUKA calculations, respectively.

the experimental data and the Monte Carlo (MC) results are normalized by the integral of the Bragg curve calculated between the entrance region and the BP. Figure 2 also indicates that the dose beyond the BP predicted by FLUKA agrees with the experimental one. The tail, as well known, is due to the lower-charge fragments produced in the projectile fragmentation. The dose in this region is mainly due to protons and He but a not negligible contribution is due to heavier fragments such as boron. Its correct estimation is demanded for a reliable determination of the dose delivered to the healthy tissues in the proximity of the treated tumor. The importance of the *nuclear effects* generally increases as a function of the beam energy (or penetration depth). For example, for a

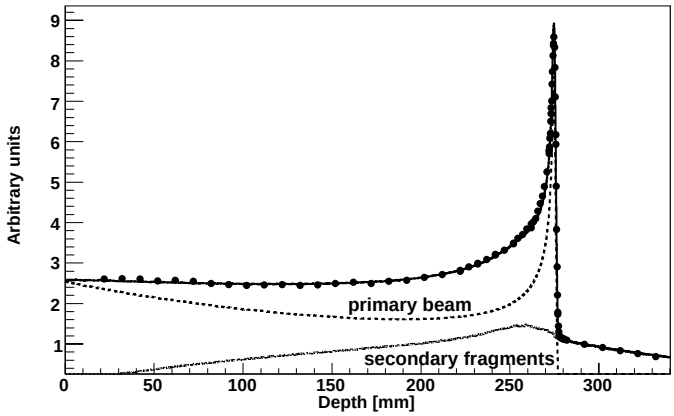

Fig. 2. – Bragg curve as a function of depth in water for a 400 MeV/n carbon beam. The points [8] and the solid line [9] represent the experimental data and the FLUKA calculations, respectively. The dose contribution from primary ^{12}C ions and secondary fragments is also reported. Both the experimental data and the MC results are normalized by the integral of the Bragg curve calculated between the entrance region and the BP because the experimental data are obtained as relative values.

200 MeV/n ^{12}C beam in water about 30% of the primary carbon ions undergo nuclear reactions and therfore, do not reach the BP whereas at 400 MeV/n already 70% (fig. 1) of the primary particles do not reach the BP [11].

The correct estimation of the mixed field in terms of particle type and particle energy is necessary not only for physical calculations but also for biologically based calculations. In fact the relative biological effectiveness (RBE) of the reaction products is different from the primary ions and has to be included in the biological calculations. To enable biological simulations taking into account the complex mixed radiation fields generated by ion beams, FLUKA can be used via a versatile interface with external biological databases.

In proton therapy, for instance, FLUKA has been used for simulating the biological features of the fully-modulated 72 MeV proton beam of the PSI therapy unit. This has been achieved interfacing the code with a biophysical model based on the assumption that the clustered DNA damage is a relevant step of the process leading to cell inactivation [12]. Simulated and experimental results with V79 cells consistently confirm that the RBE increases in the distal part of the Spread-Out Bragg peak and the peak in the biological effect is therefore shifted downstream from the physical dose peak. More recently, in order to simulate the biological effect of the carbon ion interaction with tissue, the FLUKA code has been interfaced with the Local Effect Model [13,14] developed at the Gesellschaft für Schwerionenforschung Darmstadt (GSI). The ensuing calculations have permitted to simulate the cell survival, the biological dose and the RBE after carbon ion irradiation of water phantoms simulating different cell lines. Comparisons against experimental data and TRiP (TReatment Planning for Particles [15, 16]) analytical calculations are generally in good agreement, except for the latter ones in the tail behind the BP due to the different representation of nuclear reactions. This work reported in [9] was the first step in order to study the biological effects in a clinical situation. In fact, the most interesting development that is currently under investigation is merging the clinical CT-based calculations of physical dose (described in sect. **3**) with the biological effect quantification in order to completely reproduce a clinical patient case also from the biological point of view.

3. – CT-based calculations of dose

Nowadays, dedicated or commercial treatment planning systems (TPSs) for ion therapy are essentially analytical codes based on fast performing pencil-beam algorithms. However, MC statical methods are increasingly considered powerful tools for accurate calculations of dose deposition, since they are assumed to provide a more realistic representation of the physical interactions undergone by the primary beam and the resulting secondaries. Therefore, MC re-calculations of treatment plans determined by the analytical TPSs can be very useful to investigate the accuracy of the dose calculations in critical cases sensitive to lateral scattering (especially for protons), nuclear fragmentation (especially for heavier ions), and in the presence of large density gradients, *e.g.*, due to metallic implants.

The FLUKA code has been recently upgraded for modeling part of the simulated geometry in terms of voxels, *i.e.* three-dimensional parallelepipeds all of equal dimensions with a dedicated algorithm to achieve fast tracking performances [17]. In this way it is possible to import CT data scans into FLUKA. Details on the conversion of the CT scan information into the necessary elemental composition and tissue density which are requested for the MC particle transport are described in [18, 19].

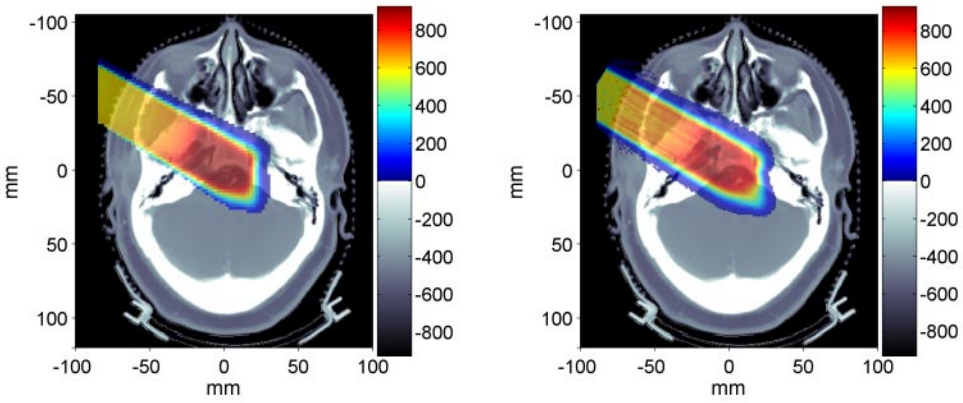

Fig. 3. – (Colour on-line) Comparison between treatment plan (left) and MC (right) calculated dose distributions for an oblique portal delivering 909 mGy to a clivus chordoma patient [20]. The color bar shows dose levels in mGy, whereas the CT numbers (black-white scale) were arbitrarily rescaled for display purposes.

An example of MC calculated dose delivery is shown in fig. 3 [20] for one single oblique proton portal of a cranial tumor patient treated at the Francis H. Burr Proton Therapy Center at Massachusetts General Hospital (MGH) Boston. At MGH a dedicated MC framework was developed to support clinical studies on PET/CT imaging after proton treatment (discussed in **4**). Patient-specific initial beam information is provided by a separate Geant4 MC calculation [21] while particle transport in the patient is performed on the planning CT using the FLUKA MC code [18-20]. The dose distribution is compared with the calculation of the commercial analytical treatment planning system (XiO, Computerized Medical Systems Inc.). The comparison between the MC calculation and the planned dose distribution generally shows good agreement in terms of lateral field extension and beam range. Differences are found in cases more sensitive to the limitations of analytical pencil beam algorithms, like in the presence of air/tissue interfaces or metallic implants [18, 19]. When normalizing both calculations to the prescribed dose delivery, minor differences are also found in terms of absolute dose values because of the different computational approach. A MC calculation in fact keeps into account a realistic composition of the patient tissue based on the stoichiometric calibration of the CT scan [22]. Differently, the commercial treatment planning system computes dose deposited to water, accounting for the patient density by means of a proper adjustment of the beam penetration depth. Hence, the former MC approach can provide a more accurate calculation of the dose deposited to tissue, especially in the presence of high-density and high-Z materials.

For carbon ions, FLUKA CT-based calculations of dose have been recently compared with the results of TRiP used in clinical routine at GSI [9]. In addition of what was already observed for protons, further deviations can be found in the fragmentation tails. These are tightly related to the different handling of the nuclear reactions. Further comparisons between the FLUKA code and the production and development versions of the TRiP treatment planning system for other patient cases are ongoing at the Heidelberg Ion Therapy Center (HIT) and will be soon reported.

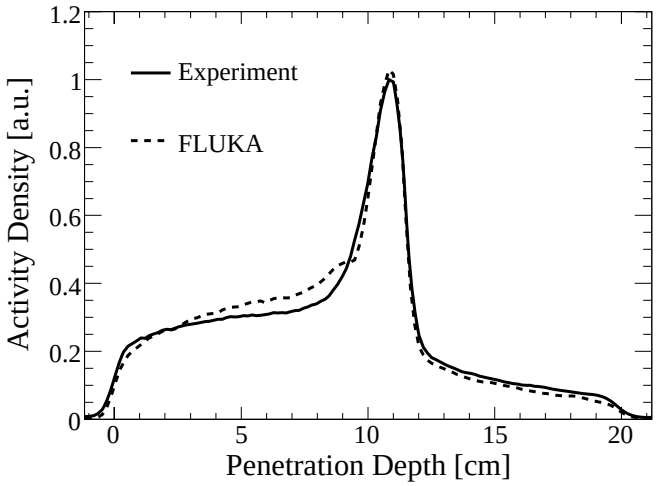

Fig. 4. – Activity measured by in-beam PET for a 260 MeV/n ^{12}C beam irradiation of a PMMA phantom. The dotted line is the result of the FLUKA simulation, the solid line shows the experimental result [24]. Both the experimental data and the MC calculations are normalized to the same area.

4. – PET therapy monitoring

Clinical exploitation of the physical advantages of ion beams for improved conformation of the dose delivery can benefit from an *in vivo*, non-invasive verification of the applied treatment and, in particular, of the beam range in the patient. Since ion irradiation produces β^+-emitters like ^{11}C and ^{15}O, PET imaging during or shortly after treatment can be used to *visualize* the delivered treatment in the patient. However, the density of activated isotopes and resulting annihilation photons is not directly proportional to the delivered dose. In order to infer useful clinical information, the expected activation can be calculated with MC tools and compared with the measured PET image. At MGH, as briefly described in sect. **3**, a MC framework was developed to support clinical studies on PET/CT imaging after proton treatment. Positron emitter distributions are obtained by internally combining FLUKA calculated proton fluence with experimental cross-sections for ^{11}C, ^{15}O, ^{13}N, ^{38}K, ^{30}P and ^{14}O yield [18, 19]. Blurring effects due to image formation and reconstruction are modeled by a convolution kernel. Promising clinical results have been presented in [23].

In proton therapy only β^+-active target fragments can be produced which approximately stay on the place where they are created. For heavier ions, the situation is more complicated due to the additional creation of β^+-active projectile fragments which still can move after their creation. In addition, due to the lack of experimental cross-section data the simulation of the activity distribution has to rely on internal nuclear models. Recent work was devoted to this topic in order to test the reliability of the new BME model [4] and to exploit recent features of FLUKA which allow the simulation of radioactive decays and transport of the emitted positrons and annihilation photons [24, 25]. An example is reported in fig. 4 where the measured β^+-activity (solid line) created in a PMMA phantom during irradiation with a 260 MeV/n ^{12}C beam is compared to a FLUKA simulation (dotted line) [24, 25].

5. – Conclusions and outlook

FLUKA applications to hadron therapy are fast growing due to the reliable nuclear models of the code, the possibility of importing patient CT scan data and the feasible coupling with external radiobiological models. Promising examples have been presented which span from physical and biological dose calculations to PET monitoring in proton and carbon ion therapy.

The FLUKA Collaboration is working on further improvements of the calculation models especially regarding a new library for low-energy neutron transport and the new BME event generator for low energy nucleus-nucleus interactions.

* * *

The work discussed here has been carried out in different collaborations with CERN, the Massachusetts General Hospital (MGH), the Heidelberg Ion Therapy Center (HIT), the Gesellschaft für Schwerionenforschung (GSI), the Forschungszentrum Dresden-Rossendorf (FZD) and the University of Pavia. This work was partially supported by INFN-CSN5 (FLUKA2 experiment).

REFERENCES

[1] Ferrari A. *et al.*, CERN 2005-10 (2005).
[2] Fassò A. *et al.*, hep-ph/0306267.
[3] Sorge H., Stöcker H. and Greiner W., *Nucl. Phys. A*, **498** (1989) 567c; Sorge H., Stöcker H. and Greiner W., *Ann. Phys. (N.Y.)*, **192** (1989) 266.
[4] Cerutti F. *et al.*, *Proceedings of the 11th International Conference on Nuclear Reaction Mechanisms, Varenna, June 12-16, 2006*, edited by Gadioli E., *Ricerca Scientifica ed Educazione Permanente, Suppl.*, **126** (2006) 507.
[5] Ferrari A. and Sala P. R., *Proceedings of the MC93 International Conference on Monte Carlo Simulation in High Energy and Nuclear Physics, Tallahassee (Florida), 22-26 February 1993*, edited by Dragovitsch P., Linn S. L. and Burbank M. (World Scientific, Singapore) 1994, p. 277.
[6] Fassò A., Ferrari A., Ranft J. and Sala P. R., *Proceedings of the 1st AEN/NEA Specialists' Meeting on Shielding Aspects of Accelerators, Targets and Irradiation Facilities (SATIF 1), Arlington (Texas), Apr. 28-29 (1994).* OECD Documents (1995), pp. 287-304.
[7] Ballarini F. *et al.*, *Adv. Space Res.*, **40** (2007) 1339.
[8] Haettner E. *et al.*, *Rad. Prot. Dos.*, **122** (2006) 485.
[9] Mairani A., PhD Thesis, University of Pavia (2007).
[10] Sommerer F. *et al.*, *Phys. Med. Biol.*, **51** (2006) 4385.
[11] Haettner E., Master of Sci. Thesis, KTM, Stockholm (2006).
[12] Biaggi M. *et al.*, *Nucl. Instrum. Methods B*, **159** (1999) 89.
[13] Scholz M. *et al.*, *Radiat. Environ. Biophys.*, **36** (1997) 59.
[14] Krämer M. and Scholz M., *Phys. Med. Biol.*, **51** (2006) 1959.
[15] Krämer M. *et al.*, *Phys. Med. Biol.*, **45** (2000) 3299.
[16] Krämer M. and Scholz M., *Phys. Med. Biol.*, **45** (2000) 3319.
[17] Andersen V. *et al.*, *Rad. Prot. Dos.*, **116** (2005) 113.
[18] Parodi K. *et al.*, *Med. Phys.*, **34(2)** (2007) 419.
[19] Parodi K. *et al.*, *Phys. Med. Biol.*, **52** (2007) 1.
[20] Parodi K. *et al.*, *J. Phys.: Conf. Ser.*, **74** (2007) 021013.
[21] Jiang H. and Paganetti H., *Med. Phys.*, **31(10)** (2004) 2811.
[22] Schneider W. *et al.*, *Phys. Med. Biol.*, **49** (2000) 459.
[23] Parodi K. *et al.*, *Int. J. Radiat. Oncol. Biol. Phys.*, **68** (2007) 920.
[24] Sommerer F., PhD Thesis, Vienna University of Technology (2007).
[25] Sommerer F. *et al.*, Ext. Abstr. IBIBAM, Heidelberg, Sept. 2007.